

Acoustic wave propagation in the solar atmosphere

V. Observations versus simulations

J. Theurer¹, P. Ulmschneider¹, and W. Kalkofen²

¹ Institut für Theoretische Astrophysik der Universität Heidelberg, Tiergartenstr. 15, D-69121 Heidelberg, Germany

² Harvard-Smithsonian Center for Astrophysics, 60 Garden St., Cambridge, MA 02138, USA

Received 28 January 1997 / Accepted 21 March 1997

Abstract. We study the evolution of spectra of acoustic waves that are generated in the convection zone and propagate upward into the photosphere, where we compare the simulated acoustic spectra with the spectrum observed in an Fe I line. Although there is no pronounced 3 min component in the spectra generated in the convection zone, there are dominant 3 min features in the theoretical spectra, in agreement with the observed spectrum. We interpret the occurrence of the 3 min features as the response of the solar atmosphere to the acoustic waves which shifts high frequency wave energy to low frequencies. We also find qualitative agreement for the acoustic power between the wave simulations and the observations.

Key words: hydrodynamics – shock waves – waves – Sun: chromosphere – Sun: oscillations

1. Introduction

In the present series of papers we investigate the response of the solar atmosphere to acoustic wave excitations. In Paper I (Sutmann & Ulmschneider 1995a) we studied the excitation and propagation of small-amplitude (linear) adiabatic waves, and in Paper II (Sutmann & Ulmschneider 1995b), the excitation of large-amplitude adiabatic waves which form shocks. Similar numerical and analytical work was carried out by Kalkofen et al. (1994). These studies show that, for monochromatic or pulse excitation, the solar atmosphere responds with oscillations in an added band of frequencies generally above 5.5 mHz (period ~ 3 min) and that, depending on the type of excitation, these 3 min oscillations usually decay after some time. Because both the monochromatic and pulse excitation happen to an atmosphere considered to be initially at rest, these 3 min oscillations could be seen as decaying transients. Yet Paper I also showed that even with very small amplitude (linear) excitations, for the stochastic wave case, the generated 3 min type oscillations did

not decay as in a switch-on effect, but were perpetually regenerated due to the stochastic nature of the excitation (cf. Fig. 14 of Paper I). In Paper II, in addition to monochromatic or pulse excitations, perturbations by four different types (Gaussian, box, exponential and stochastic) of acoustic wave spectra were studied. It was found that these perturbations led to 3 min oscillations which over the time span of the calculations (~ 2500 s) did not decay. Below we will refer to the 3 min oscillations near the acoustic cutoff as “resonance oscillations”.

The 3 min oscillations are also a prominent observational signal in the outer solar atmosphere. In the quiet solar atmosphere they are seen in the interior of supergranulation cells: in the Ca II H and K lines, in $H\alpha$ and in the Ca II infrared triplet lines as well as in other, lower-lying photospheric and chromospheric lines. For detailed reviews and discussions of the 3 min oscillations see Deubner (1991), Fleck & Schmitz (1991), Rutten & Uitenbroek (1991), Rossi et al. (1992), Carlsson & Stein (1994), Rutten (1995, 1996), Steffens et al. (1995) and Al (1996).

The analytical work of Paper I will be extended to include the excitation of linear, adiabatic waves by a pulse and by acoustic spectra (Sutmann et al. 1997; Paper III). For similar analytical work see Schmitz & Fleck (1995). Recently (Theurer et al. 1997; Paper IV) we investigated the excitation of the solar atmosphere by large-amplitude, non-adiabatic acoustic spectra. In Paper II the excitations with acoustic spectra could not be carried out over extended times because due to shock formation and shock heating the adiabatic waves generate secular changes of the atmospheric structure with temperatures which perpetually rise with time. The non-adiabatic treatment in Paper IV avoids this problem. Here the excitation leads to a dynamical equilibrium between shock heating and radiative cooling, which results in a time-independent mean atmosphere, where the wave excitation could now be carried out up to arbitrarily large times.

As already suspected in Paper II these calculations showed that the 3 min type resonance oscillations near the acoustic cutoff now remain a permanent, non-decaying feature of the wave spectrum and that these 3 min “resonances” became more and more prominent with height. It was found that regardless of

the initial shape of the acoustic wave spectrum (Gaussian or stochastic), introduced at $z = 0$ km into the atmosphere, the resulting spectrum at a height of $z = 2000$ km consisted almost exclusively of components in the 3 min band. Moreover, after about 500 s the spectra at a given height no longer showed any time dependence.

In an attempt to simulate the observed 3 min oscillations, in particular, those observed in the K_{2v} bright points in the interior of supergranulation cells, Carlsson & Stein (1994, 1995) excited the oscillations using the observed velocity variation of a low-lying Fe I line (Lites et al. 1993). They obtained good agreement of observed and simulated H line profiles as well as of the time delay between the oscillations at the Fe line and the H line.

Similar work by Cheng & Yi (1996) but employing a different numerical code has recently been carried out. They introduced high-frequency acoustic wave power in addition to the observed spectrum and found that high-frequency waves did not contribute to the 3 min band at chromospheric heights, concluding that the pronounced power in the 3 min band must already be present at the site of generation of the waves. This claim has to be viewed with some caution since their code, which is different from that of Carlsson & Stein, does not have an adaptive mesh capability and thus does not allow the treatment of shocks and hence the limiting shock strength behaviour and the merging of shocks, that is, of effects we find critical for the generation of power near the acoustic cutoff from high-frequency waves. However, the question remains open whether the 3 min oscillations are introduced into the acoustic spectrum at the height where the waves are generated, or added later by the atmosphere.

In recent years it has become clear that the acoustic energy generation in the convection zones of late-type stars is strongly tied to the Kolmogorov turbulent energy spectrum, which is now well supported for the solar convection zone by numerical simulations (Cattaneo et al. 1991) as well as by high-resolution observations (Muller 1989, Nesis et al. 1993). For a discussion see Musielak et al. (1994). On the basis of this turbulent energy spectrum, the wave generation calculations using the Lighthill-Stein theory of sound generation produce acoustic spectra that are smooth and have a single broad peak in the 1 min band, i.e., most of the acoustic power is found at frequencies much higher than the 3 min band (Figs. 3 and 4). This is due to the property of the Kolmogorov turbulent cascade in its inertial range (discussed below) of extending to frequencies of at least 100 Hz under adiabatic conditions when viscosity limits the cascade, or to frequencies of at least 300 mHz when radiative exchange between adjacent bubbles limits the cascade.

Thus one must reconcile the theory showing the generation of a high-frequency wave spectrum without a noticeable 3 min feature with the observations which show a low-frequency spectrum dominated by the 3 min band. The aim of the present work is to find an answer to this problem. A possible answer is suggested by the results of the previous papers of this series and by the work of Kalkofen et al. (1994) showing that 3 min oscillations can be the response of the atmosphere to wave excitations. We will argue that the 3 min component is a feature that is added by the atmosphere to the acoustic spectrum by shifting power

from high frequencies to low frequencies during the propagation of the waves from the convection zone to the photosphere.

In our previous work we found two ways by which such a shift is accomplished. Fig. 14 of Paper I shows that already for a wave excitation with very small amplitude, resulting from an acoustic spectrum with a stochastically changing wave period, one obtains 3 min type resonance oscillations which continuously get regenerated. The second way, as shown in Paper IV, is that acoustic wave spectra with larger amplitudes lead to shock formation and shock merging, which generates resonance oscillations. In both cases the stochastic nature of the acoustic wave spectrum leads to oscillations which persist in time.

Note that in our computations it is necessary to distinguish between the quiet interior of supergranulation cells and the K_{2v} bright points that are embedded in it. The work reported here concerns mainly the oscillations in the quiet background of the cell interior and not those in the K_{2v} bright points (cf. Kalkofen 1996), where the periods tend to be somewhat longer than those found in this investigation.

In order to test the hypothesis of the transfer of power from high to low frequencies we have made a number of simplifications, such as assuming adiabatic conditions for the atmospheric wave calculations and neglecting effects of the Earth's atmosphere as well as instrumental effects when comparing our results with the observations. These simplifications will be removed in subsequent work. Sect. 2 outlines the numerical methods, Sect. 3 presents the results and Sect. 4 gives the conclusions.

2. Method

2.1. Initial wave spectrum

For the treatment of the acoustic wave spectrum we follow Paper II. At the lower boundary of the computational domain, velocity fluctuations are prescribed for the piston. The frequency spectrum has $N + 1 = 101$ partial waves at the frequencies $\omega_n = 2\pi\nu_n$, which are spaced 0.5 mHz apart; and $\nu_1 = 4.0$ mHz. The piston velocity, v , is prescribed by the superposition

$$v(t) = \sum_{n=0}^N u_n \sin(\omega_n t + \varphi_n) \quad , \quad (1)$$

where u_n is the velocity amplitude of a partial wave and φ_n an arbitrary but constant phase angle. Since the velocity amplitude at the piston is small the mechanical energy flux, F_A , can be written using linear theory as

$$F_A = \frac{1}{T} \int_0^T \rho c \sum_{n=0}^N (u_n \sin(\omega_n t + \varphi_n))^2 \cos \alpha_n dt, \quad (2)$$

where T is an arbitrary but sufficiently long time for the averaging, ρ is the density and α_n the phase shift between velocity and pressure fluctuations, which is given by

$$\alpha_n = \arctan \left(\frac{\omega_A}{\sqrt{\omega_n^2 - \omega_A^2}} \right) \quad , \quad (3)$$

where $\omega_A = \gamma g/(2c)$ is the acoustic cut-off frequency at the bottom of the atmosphere. We normalize the velocity amplitudes to the prescribed acoustic energy flux F_A and obtain

$$u_n = q \sqrt{\frac{F_A}{\rho c}} f(\omega_n) , \quad (4)$$

where q is a normalization factor and $f(\omega_n)$ the spectral distribution function. The normalization factor q is chosen such that upon introduction of Eqs. (3) and (4) into Eq. (2) the prescribed flux F_A is obtained.

2.2. Kolmogorov turbulent cascade, high frequencies

The initial acoustic wave spectrum is not well known since it results from the turbulent energy spectrum of the solar convection, which is poorly known. Musielak et al. (1994) argued on the basis of observations and numerical convection simulations, that the turbulence in the solar convection zone must have a Kolmogorov type energy spectrum in which the wave numbers near $k_0 = 2\pi/H$, where H is the local scale height, represent the energy-containing eddies that start the turbulent cascade.

Since it has been suggested frequently on the basis of observations that high-frequency acoustic waves not only do not have any influence on chromospheric oscillations but do not even exist, we briefly discuss here the high-frequency part of the turbulent energy spectrum, which is the origin of the high-frequency part of the acoustic wave spectrum.

In homogeneous isotropic turbulence, the inertial forces break up larger turbulent eddies into smaller ones. A turbulent flow field can be described by three characteristic quantities, namely, the density ρ , the bubble size $l_k = 2\pi/k$, and the mean velocity u_k of such bubbles, where k is the wavenumber. It is easily seen that from these three quantities only one combination can be formed for the heating rate (in $\text{erg cm}^{-3} \text{ s}^{-1}$), namely:

$$\Phi_k = \rho \frac{u_k^3}{l_k} . \quad (5)$$

Since in the turbulent cascade the energy is passed on from large to small bubbles the heating rates must satisfy the condition $\Phi_{k0} = \Phi_{k1} = \Phi_{k2} = \dots = \text{const}$, where the wave numbers, k_0, k_1, k_2, \dots , represent a series of bubbles of decreasing size. As the mean density ρ is unaffected this implies that

$$u_k \sim l_k^{1/3} . \quad (6)$$

Equation (6) is referred to as the *Kolmogorov law*. The range $l_{k0} \dots l_{kn}$ of validity of this law is called the *inertial range*. It ends when the bubble size l_k is so small that viscous heating becomes important, that is, when the turbulent heating rate becomes equal to the viscous heating rate, i.e.,

$$\eta \left(\frac{du}{dz} \right)^2 = \rho \frac{u_{k0}^3}{l_{k0}} . \quad (7)$$

For the energy-carrying eddies at the beginning of the cascade we have $u_{k0} \approx 1 \cdot 10^5 \text{ cm/s}$, $l_{k0} \approx 1.5 \cdot 10^7 \text{ cm}$, $\rho \approx 3 \cdot$

10^{-7} g/cm^3 . With $(du/dz)^2 = (u_k/l_k)^2$ and Eq. (6) one finds for the size of the smallest bubbles

$$l_k = \left(\frac{\eta l_{k0}^{1/3}}{\rho u_{k0}} \right)^{3/4} . \quad (8)$$

Using $\eta \approx 5 \cdot 10^{-4} \text{ dyn s/cm}^2$ we obtain $l_k = 2.9 \text{ cm}$ and $u_k = 290 \text{ cm/s}$ for the smallest bubbles, which gives $\nu_k = u_k/l_k = 99 \text{ Hz}$ for the maximal frequency.

This limit of the turbulent cascade is valid only under adiabatic conditions. If radiation is considered, neighboring bubbles will exchange energy. If the smallest size of the bubbles is limited by radiative exchange, it will be given by the optical diameter $\tau = l_k \kappa \rho = 0.1$. Using the analytic representation $\kappa = 1.38 \cdot 10^{-23} p^{0.738} T^5 \text{ cm}^2/\text{g}$ for the Rosseland grey opacity (cf. Ulmschneider et al. 1978) and the values $T = 8300 \text{ K}$ and $p = 2 \cdot 10^5 \text{ dyn/cm}^2$ for the temperature and pressure, we obtain $l_k = 7.5 \cdot 10^4 \text{ cm}$ and $u_k = 1.7 \cdot 10^4 \text{ cm/s}$ for the smallest bubbles with a frequency of $\nu_k = 230 \text{ mHz}$. This shows that the acoustic spectrum extends to relatively high frequencies at the point of its generation and confirms that short period acoustic waves are indeed present in stellar atmospheres.

2.3. Kolmogorov turbulent cascade, low frequencies

While the high-frequency part of the turbulent energy spectrum appears to be reasonably well established, there is considerable uncertainty about the low-frequency part. Musielak et al. (1994) pointed out that, at low wave numbers, observations e.g. by Muller (1989) show that the velocity power still increases with decreasing wave number k although with a smaller slope. To take into account a deviation from the classical Kolmogorov spectrum for wave numbers $k < k_0$, Musielak et al. considered three possible forms of the energy spectrum, which for $k > k_0$ has the Kolmogorov shape but for lower wave numbers has different dependences on k . Their spectra, called extended, broadened and raised Kolmogorov spectra, are given by their Eqs. (35) to (37) and are displayed in their Fig. 1.

Since we cannot ignore the uncertainty in the turbulent energy spectrum we selected the two most extreme cases studied by Musielak et al. (1994) and computed the acoustic energy generation on the basis of the extended (eKmG) and of the raised Kolmogorov (rKmG) spectrum, both with a modified Gaussian frequency factor. The spectral shape of the resulting acoustic spectra, $f(\omega)$, is shown in Figs. 4 and 8 of Musielak et al. (1994). Taking a mixing-length parameter of $\alpha = 2$ we have a total acoustic flux of $F_A = 1.97 \cdot 10^8$ and $8.75 \cdot 10^7 \text{ erg cm}^{-2} \text{ s}^{-1}$ for the eKmG and rKmG spectra, respectively. Spline-fitted versions of the selected spectra $f(\omega)$ are shown in Figs. 3 and 4 below.

These spectra are generated in a very narrow height range around $z = -130 \text{ km}$ in the convection zone, where the convective velocity u has its maximum (see Fig. 7 of Musielak et al. 1994). The reason for the localization of the acoustic energy generation in a thin layer is the sensitive u^8 dependence of

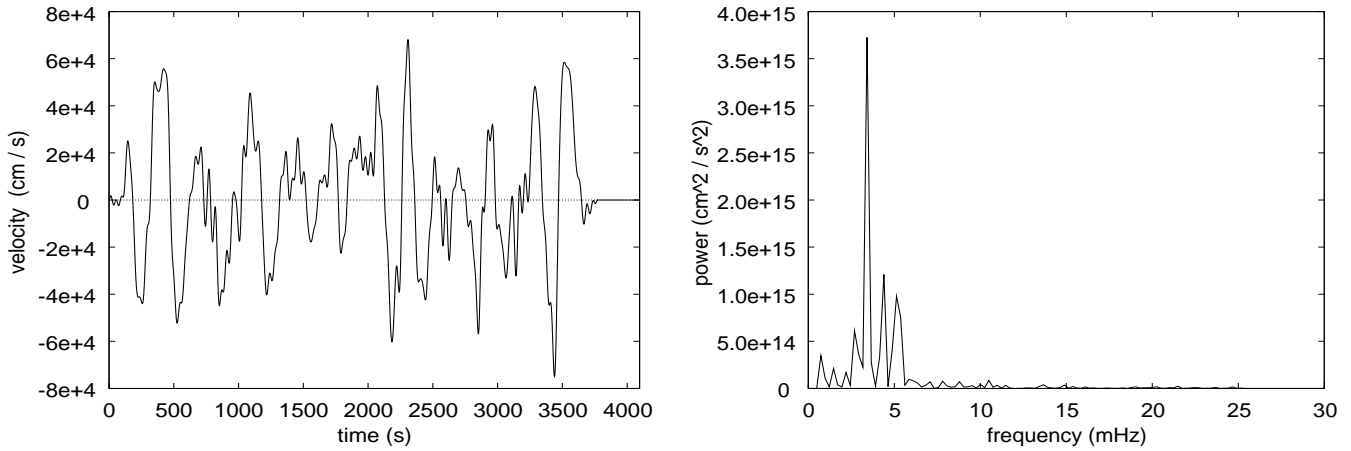


Fig. 1. Velocity (left panel) and power spectrum (right panel) in an Fe I line observed by Lites et al. (1993). Some high frequency components have been filtered out, the line is formed roughly at a height of $z = 250$ km.

the quadrupole sound generation rate on the convective velocity u . Such a height ($z \approx -140$ km) of the maximum acoustic energy production has also been found by Kumar (1994). Moreover, it is found (Steffen 1992) that a significant difference of the mixing-length approach as compared with the numerical convection computations is that in the latter, the maximum convective velocity occurs about 100 km deeper, which translates into a layer of maximum acoustic energy generation, roughly in the range $z = -150$ km to -250 km. We thus feel that a value $z = -160$ km is a reasonable choice.

As to the choice of the mixing-length parameter α , we point out that currently the larger values of $\alpha = 1.7$ to 2.0 are preferred (Kumar 1994, Musielak et al. 1994) and that a value of $\alpha = 2.0$ is indicated by a comparison of the peak value of the convective velocity in mixing-length calculations with that in time-dependent hydrodynamic convection simulations (Steffen 1992), as well as by a careful fitting of evolutionary tracks of the Sun with its present properties L , T_{eff} and age (Hünsch & Schröder 1996, Schröder & Eggleton 1996).

2.4. Wave calculation, atmospheric model

We follow the development of the acoustic wave spectrum with a hydrodynamic code where for simplicity we assume adiabatic conditions. The details of the wave computation have been described in Papers I and II. The time-dependent hydrodynamic equations are solved using the method of characteristics. We follow the development of the originally linear wave, introduced by specifying the piston velocity using Eq. (1) at the bottom of the atmosphere, up to the point of shock formation and beyond. Shocks are treated as discontinuities and are allowed to grow to arbitrary strength and to merge.

We consider an atmospheric slab extending from $z = -160$ km to a height of 1700 km and use a total of 300 grid points with a spacing of 6.2 km. In addition to the fixed number of regular grid points there is an arbitrary number of shock

points, which are allowed to move between the regular points according to the speed of the shocks.

For the atmospheric model we take model C of Vernazza et al. (1981). Since for both mixing-length models and numerical convection zone models the maximum of the convective velocities occurs below their lowest point, at $z = -75$ km, we extended this model for a few points by fitting a solar convection zone model similar to those described by Ulmschneider et al. (1996).

2.5. The observed frequency spectrum

For the observed velocity spectrum we use the velocity fluctuations of an Fe I line formed at $z = 250$ km observed by Lites et al. (1993). The original data consist of a time series of Doppler velocities at 5 adjacent spatial points along the slit position through the interior of a supergranulation cell. The data were low-pass filtered, at 15–25 mHz to remove noise, and apodized. They were provided to us by Mats Carlsson (1995, private communication). Each time series consists of 754 measurements at equal time steps of 5 s. This velocity spectrum is shown in Fig. 1, with the velocity fluctuations in the left panel and Fourier spectrum in the right panel. To obtain a set of data points consisting of a number of points that is equal to a power of 2, for the Fast Fourier Transform, we have augmented the data set with zeros up to 4096 s, as indicated in Fig. 1. Similar although noisier data of a Na I line, also by Lites et al. (1993), were used by Cheng & Yi (1996, their Fig. 2).

The dominant feature in Fig. 1 is the well known solar 5 min oscillation at 3.3 mHz. This feature is due to trapped subphotospheric acoustic eigenmodes involving the entire Sun and thus cannot be expected to be reproduced by our local one-dimensional simulation. Our focus of interest rather is the 3 min oscillations in the 5 to 6 mHz range which we want to explain as the result of atmospheric resonance oscillations.

For the comparison of our simulations with solar data we note also the properties of the observed velocity power spectrum

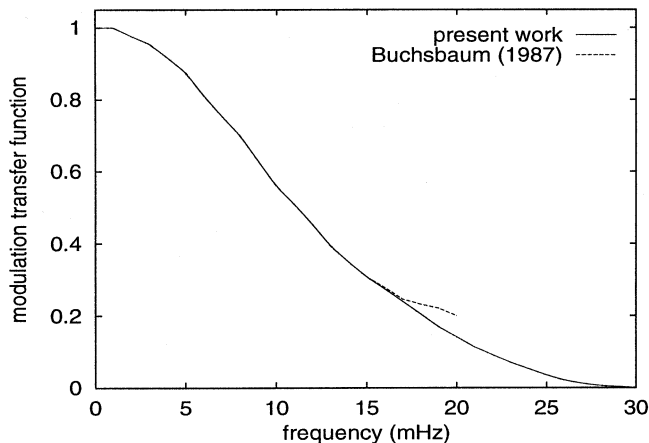


Fig. 2. Modulation transfer function after Buchsbaum (1987) for the Fe 5930 Å line.

at H_3 in the core of the H line by Lites et al. (1993, their Fig. 6), which shows peaks at 5 mHz, 6.5 mHz and 7 mHz. These observations are from the interior of supergranulation cells and thus both the quiet background and the K_{2v} bright points contribute to the spectrum. For the K_{2v} bright points, the observations of v. Uexküll & Kneer (1995) indicate that their emission is spatially and temporally intermittent. This property is reproduced by a model with impulsive excitation of waves (Kalkofen 1996). Excitation by the turbulence of the convection zone cannot reproduce the observed intermittence. The work reported here therefore concerns waves in the quiet cell interior. Nevertheless, the turbulence-generated waves may also contribute to some bright point heating.

2.6. The modulation transfer function

A direct comparison of observed velocity spectra with theoretical spectra is not easily achieved since any velocity event occurring on the Sun is affected by seeing because of the Earth's atmosphere, by instrumental degradation and, most of all, by the fact that the observed spectral lines have a width Δz_W of their contribution function which extends over at least two scale heights. It is well known that velocity fluctuations with wavelengths $\lambda \ll \Delta z_W$ do not contribute to Doppler shifts of the line core but instead to line-broadening. Thus, when the frequency approaches the critical value where $\lambda \approx \Delta z_W$, the velocity fluctuations seen by Doppler shifts abruptly decrease and approach zero for higher frequencies. The ratio of the actual velocity to the velocity seen as a Doppler shift, v/v_{Doppler} , which is a function of the acoustic frequency, is called the modulation transfer function (see also Deubner et al. 1988, Ulmschneider 1990). It is obtained by computing propagating sound waves, simulating the spectral lines and comparing the Doppler shifts of the absorption core of the line with the actual velocities in the line-forming region.

In this exploratory investigation we avoid such detailed line simulations and take published values of the modulation transfer function. Fig. 2 shows a typical case from Buchsbaum (1987)

for the Fe 5930 line, which is formed at a height of $z = 250$ km. The function has been extended arbitrarily to 30 mHz and assumed to be zero above this frequency.

At this point we want to emphasize that because of the modulation transfer function we do not consider simulations like those of Carlsson & Stein (1994, 1995) and Cheng & Yi (1996) to be very realistic, because they use a spectrum observed from Earth as an input for their computations, leaving out the largest part of the high frequency acoustic spectrum which theoretically must be present at their lower boundary as discussed above. Moreover in similar computations as those by the mentioned authors we find strong emission cores in the IRT lines of Ca II. These emission cores, which are also found for the Vernazza et al. (1981) solar models if microturbulence is neglected or only a small amount of microturbulence is used, are not observed. Inclusion of a large amount (see Vernazza et al.) of microturbulence can suppress these Ca II IRT emission cores. This microturbulence could possibly be the broad high frequency band neglected by the above authors.

3. Results

With our hydrodynamic code and using the spectra described above we have simulated the propagation of acoustic waves from their generation height at $z = -160$ km up into the photosphere. Figs. 3 and 4 show the resulting acoustic spectra at $z = -160$ km, 250 km and 500 km. The left-hand columns of these figures show the velocity fluctuations at the respective heights. It is seen that the velocities at any given height vary in a random way. The middle columns display the raw acoustic spectra while the right-hand columns show them with the modulation transfer function applied. Note that for the eKmG spectrum there is a much larger high-frequency contribution to the acoustic spectrum than for the rKmG spectrum. In addition, due to our choice of frequency spacing of the 101 partial waves it is seen that the acoustic spectra extend from 4 mHz to 54 mHz.

Although the high-frequency filtering effect of the modulation transfer function cannot be observed at the generation height (-160 km) we have applied the transfer function to the input spectrum as well in order to show the magnitude of this effect. Note the difference in the frequency scales of the figures in the right-hand columns as compared to the middle columns.

Comparing the spectra at heights of 250 km and 500 km with those at -160 km it is seen that the spectra progressively gain low-frequency components with height; this is best seen in the figures with the modulation transfer function applied. The spectra without the modulation transfer function retain a considerable contribution by high-frequency components and even largely their initial shape. But with increasing height, as already found in Paper IV, the initial spectral shape is progressively lost in favour of a spectrum with an increasingly dominant 3 min band.

A comparison of Figs. 1 and 3 shows rough agreement, but our simulations have more high-frequency power than the observations. But we should perhaps not overemphasize the differences between observation and theory in this exploratory calcu-

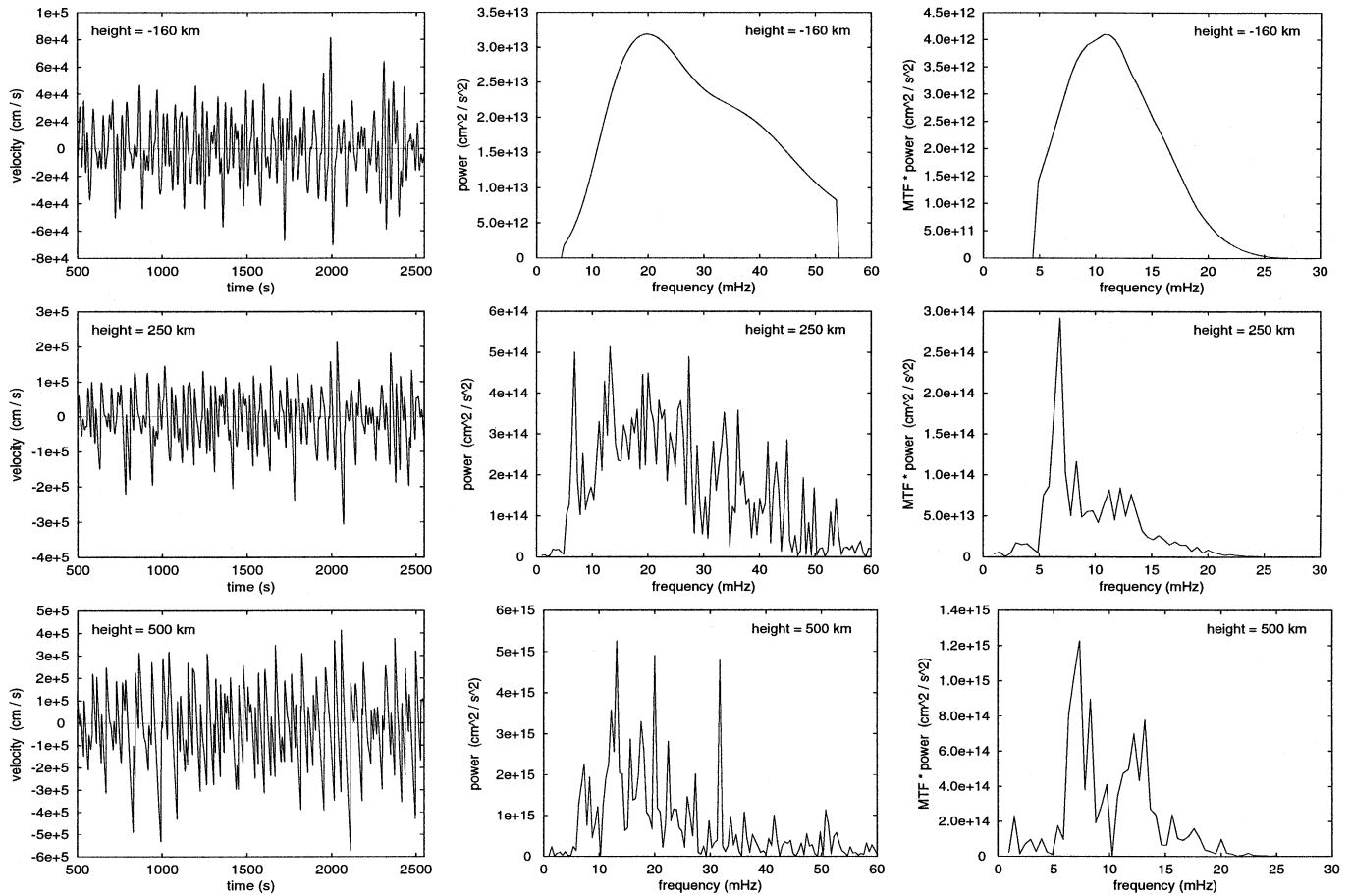


Fig. 3. Velocities (left column), power spectra without (middle column) and power spectra with the applied modulation transfer function at heights $z = -160, 250$ and 500 km (from top to bottom). The spectrum at $z = -160$ km is from a theoretical sound generation calculation using the *extended Kolmogorov* (eKmG) turbulent energy spectrum in the solar convection zone. The acoustic spectrum has a total energy flux of $F_A = 1.97 \cdot 10^8$ erg $\text{cm}^{-2} \text{s}^{-1}$.

lation because of our rather simplistic approach where in the theoretical treatment we neglected radiative damping, the detailed evaluation of the modulation transfer function and seeing and instrumental effects, and where in the treatment of the observations we made several simplifying assumptions. The important result from the comparison of Figs. 3 and 4 with Fig. 1 is that there is a dominant peak near 3 min in both the simulations and the observations and that this peak is not present in the initial acoustic spectra at the generation height of -160 km. This indicates that the generation of the 3 min waves in the simulations is a property of the atmosphere.

It is remarkable that the low-frequency spectrum with a peak at 7 mHz derives from acoustic spectra peaked at high frequencies (of ≈ 14 to 20 mHz). This result is at variance with the finding of Cheng & Yi (1996) who claim that short-period waves play no role in the generation of the observed spectrum dominated by the 3 min peak, a signal they believe to be necessary at site of the acoustic wave generation.

As in Paper IV, we have monitored the heights of shock formation and of shock merging. In computations extending to a time of 5000 s we found that, respectively, 190 and 150 shocks

were generated at heights concentrated between 200 to 400 km and between 300 to 500 km for the eKmG and rKmG spectra. In addition, respectively, 80 and 60 shock mergings occurred at heights above 500 and 600 km for the eKmG and rKmG spectra. Temperature minima were generated at 350 to 450 km in these calculations with temperatures reaching 22000 K at 1500 km height in both cases.

In our computations we also monitored the total acoustic flux as function of height. We found that up to about $z = 500$ km height one essentially had flux conservation with the flux decreasing by less than a factor of two, while above this height the flux decreased rapidly due to the dissipation by fully developed shocks. In this height interval of about 660 km, the density decreased by more than two orders of magnitude, leading to a large amplitude growth of the acoustic waves.

Another important result is that the acoustic fluxes computed on the basis of our simulations produce magnitudes in the power spectra ($3 \cdot 10^{14}$ to $1.2 \cdot 10^{15}$ cm^2/s^2 for the eKmG and $5 \cdot 10^{14}$ to $3.5 \cdot 10^{15}$ cm^2/s^2 for the rKmG spectrum) that are in rough agreement with the magnitude of the observed power ($1 \cdot 10^{15}$ cm^2/s^2) for frequencies greater than 4 mHz. This is

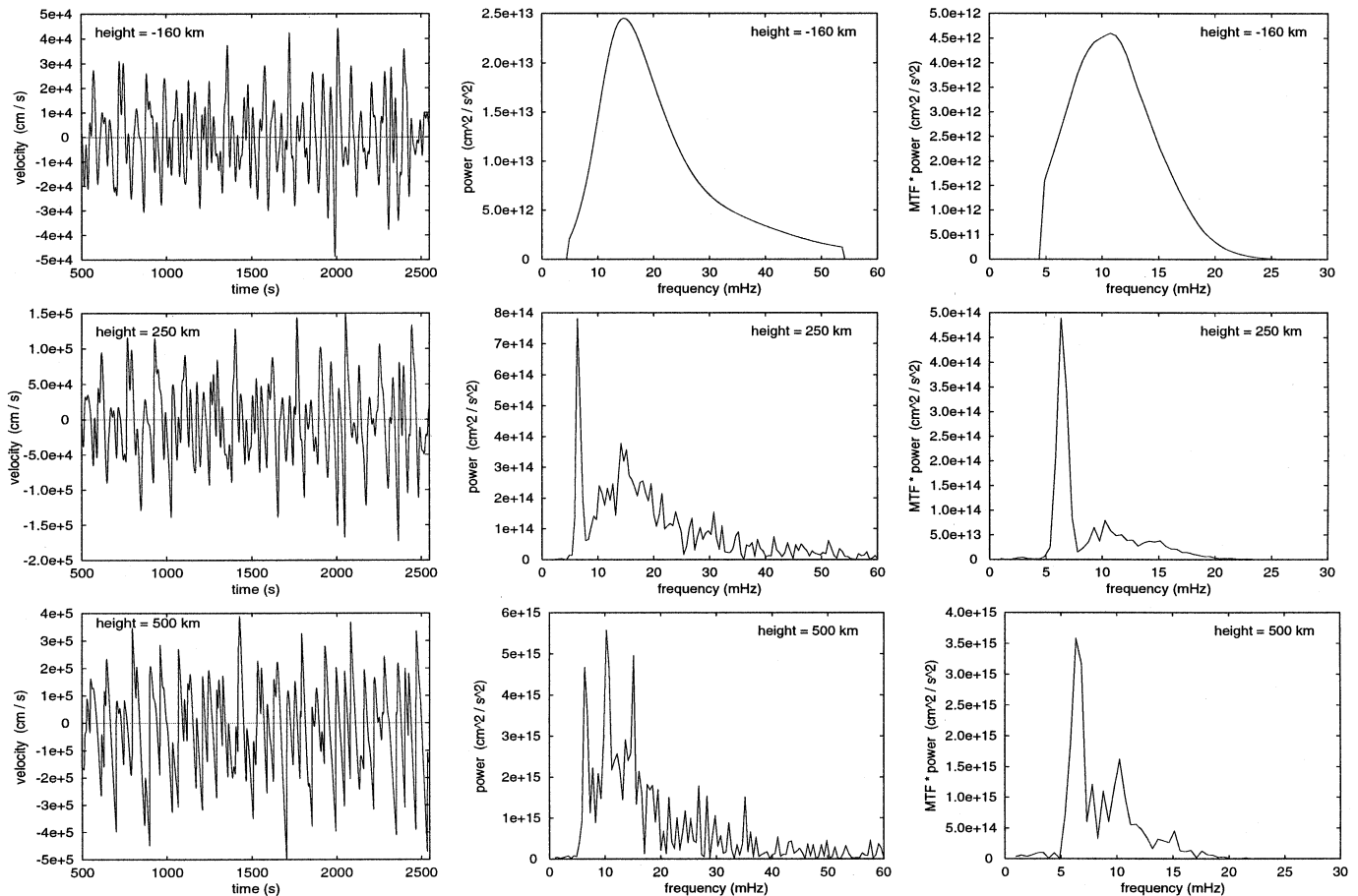


Fig. 4. Velocities (left column), power spectra without (middle column) and power spectra with the applied modulation transfer function at heights $z = -160, 250$ and 500 km (from top to bottom). The spectrum at $z = -160$ km is from a theoretical sound generation calculation using the *raised Kolmogorov* (rKmG) turbulent energy spectrum in the solar convection zone. The acoustic spectrum has a total energy flux of $F_A = 8.75 \cdot 10^7 \text{ erg cm}^{-2} \text{ s}^{-1}$.

seen when comparing Figs. 3 and 4 with Fig. 1 and indicates rough overall agreement between the theoretical concepts of sound generation by turbulent convection and observation. This suggests that we might be able to use the observations of acoustic velocity fluctuations to determine critical physical quantities like the maximum convective velocities, the depth of the maximal flow velocity and the efficiency factors in the Lighthill-Stein theory of sound generation. The result moreover shows that a more refined theoretical simulation and a more detailed comparison with observation is urgently needed.

Theoretically the magnitude of the convective velocity appears to be not overly uncertain, as the comparison of numerical convection calculations with the mixing-length calculations by Steffen (1992) shows. He found that mixing-length computations provide maximum velocities of 2.0, 2.6 and 3.1 km/s for $\alpha = 1, 2$ and 3, respectively, while his numerical convection calculations show maximum convective velocities of 2.8 km/s. A greater difference between the mixing-length results and his numerical convection simulations (which include radiation) is that in the former the convective velocities go to zero at the solar surface, while in the latter, due to the granular motion, the veloc-

ities remain finite into the photosphere, where they decrease to a minimum value of 1.2 km/s. Such motions would normally generate acoustic flux were it not for the u^8 dependence, which ignores all velocities except those close to the velocity maximum. Another significant difference of the mixing-length approach as compared with the numerical convection computations, as mentioned above, is that in the latter (Steffen 1992) the maximum convective velocity occurs about 100 km deeper. This might allow the acoustic spectrum to show a stronger 3 min component because of the greater distance to the photosphere.

4. Conclusions

Using adiabatic wave calculations we have followed the development of acoustic wave spectra from their generation height at $z = -160$ km in the solar convection zone, up into the photosphere, where we have compared them with observed spectra. 1. We find that the acoustic spectra generated by the turbulence of the convection zone do not have a pronounced peak in the 3 min band. Instead, the acoustic spectra based on the extended (eKmG) and raised (rKmG) Kolmogorov spectra of turbulent

convection and computed with convective velocities using the mixing-length theory with a mixing length parameter of $\alpha = 2.0$ have single peaks at high frequency, at 20 and 14 mHz, respectively.

2. The acoustic spectra in the simulation acquire a predominant 3 min component after the propagation of the waves from the generation height at -160 km into the photosphere at 250 or 500 km.

3. Up to these heights of 250 to 500 km the total acoustic flux is essentially conserved, decreasing by less than a factor of two. This shows that the shift from a high to a low frequency spectrum is a true shift of the wave energy.

4. The theoretical spectra are in fair agreement with the spectrum observed in an Fe I line at $z = 250$ km height after correction using a modulation transfer function, which suppresses high-frequency spectral components that are unobservable in the Doppler effect due to the finite width of the line contribution function.

Acknowledgements. We are grateful to the DFG, to NASA and NATO for support. We are also very grateful to F.-L. Deubner, S. Steffens and F. Pijpers for comments on an earlier version of the manuscript.

References

- Al N., 1996, Ph. D. thesis, Univ. Göttingen, Germany
- Buchsbaum G., 1987, Diplom thesis, Univ. Würzburg, Germany
- Carlsson M., Stein R.F., 1994. In: Carlsson M. (ed.) Proc. Oslo Mini-Workshop at Institute of Theoretical Astrophysics, Chromospheric Dynamics, p. 47
- Carlsson M., Stein, R.F., 1995, ApJ 440, L29
- Cattaneo F., Brummell N.H., Toomre J., Malagoli A., Hulbert N.E., 1991, ApJ 370, 282
- Cheng Q.-Q., Yi Z., 1996, A&A 313, 971
- Deubner F.-L., 1991. In: Ulmschneider P., Priest E.R., Rosner R. (eds.) Mechanisms of Chromospheric and Coronal Heating. Springer, Berlin, p. 6
- Deubner F.-L., Reichling M., Langhanki R., 1988. In: Christensen-Dalsgaard J., Frandsen S. (eds.) IAU Symp. 123, Advances in Helio- and Asteroseismology, p. 439
- Fleck B., Schmitz F., 1991, A&A 250, 235
- Hünsch M., Schröder K.-P., 1997, A&A 309, L51
- Kalkofen W., 1996, ApJ 468, L69
- Kalkofen W., Rossi P., Bodo G., Massaglia S., 1994, A&A 284, 976
- Kumar P., 1994, ApJ 428, 827
- Lites B.W., Rutten R.J., Kalkofen W., 1993, ApJ 414, 345
- Muller R., 1989. In: Rutten R.J., Severino G. (eds.) Solar and Stellar Granulation. Kluwer, Dordrecht, p. 101
- Musielak Z.E., Rosner R., Stein R.F., Ulmschneider P., 1994, ApJ 423, 474
- Nesis A., Hanslmeier A., Hammer R., et. al., 1993, A&A 279, 599
- Rossi P., Kalkofen W., Bodo G., Massaglia S., 1992. In: Giampapa M.S., Bookbinder J.A. (eds.) Proc. Seventh Cambridge Workshop, Cool Stars, Stellar Systems and the Sun. ASP Conf. Series 26, p. 546
- Rutten R.J., 1995. In: Hoeksema J.T., Domingo V., Fleck B., Battrock B. (eds.), Proc. 4th SOHO Workshop Helioseismology. ESA SP-376, p. 151
- Rutten R.J., 1996. In: Strassmeier K.G., Linsky J.L. (eds.) IAU Symp. 176, Stellar Surface Structure. Kluwer, Dordrecht, p. 385
- Rutten R.J., Uitenbroek H., 1991, Solar Physics 134, 15
- Schmitz F., Fleck B., 1995, A&A 301, 483
- Schröder K.-P., Eggleton P.P., 1996, Reviews in Modern Astronomy 9, 221
- Steffen M., 1992, Habilitation thesis, Univ. Kiel, Germany
- Steffens S., Deubner F.-L., Hofmann J., Fleck B., 1995, A&A 302, 277
- Sutmann G., Ulmschneider P., 1995a, A&A 294, 232 (Paper I)
- Sutmann G., Ulmschneider P., 1995b, A&A 294, 241 (Paper II)
- Sutmann G., Musielak Z.E., Ulmschneider P., 1997, A&A (submitted) (Paper III)
- Theurer J., Ulmschneider P., Cuntz M., 1997, A&A (in press) (Paper IV)
- Ulmschneider P., 1990. In: G. Wallerstein (ed.) Proc. Sixth Cambridge Workshop, Cool Stars, Stellar Systems, and the Sun. ASP Conf. Series 9, San Francisco, p. 3
- Ulmschneider P., Schmitz F., Kalkofen W., Bohn H.U., 1978, A&A 70, 487
- Ulmschneider P., Theurer J., Musielak Z.E., 1996, A&A 315, 212
- Vernazza J.E., Avrett E.H., Loeser R., 1981, ApJS 45, 635
- von Uexküll M., Kneer F., 1995, A&A 294, 252